Sensitivity of Longwave Fluxes to Clouds and Meteorology: Establishing Uncertainties for GEWEX SRB Longwave

J. Colleen Mikovitz[1], Paul W. Stackhouse[2], Jr., Taiping Zhang[1] , Stephen J. Cox[1] and Shashi K. Gupta[1]

[1]SSAI, Inc., Hampton, VA, USA
[2]NASA Langley Research Center, Hampton, VA, USA

1. Introduction

The NASA/GEWEX (Global Energy and Water Exchanges project) Surface Radiation Budget (SRB) project produces longwave and shortwave radiative fluxes for the surface and top-of-atmosphere (TOA) (see, Stackhouse et al., 2011). The primary inputs of cloud and meteorology data have been undergoing improvements in quality and spatial and temporal resolution.

Changes in the inputs and algorithm are as follows:
- Synchronized algorithm with version used by NASA CERES (Rose et al. 2006).
- Atmospheric aerosols were added.
- Beta version of ISCCP H cloud properties used.
- Beta version of ISCCP nnHIRS temperature and humidity used.
- Usage of a newly derived Princeton land surface temperature and diurnal Seaflux sea surface temperature for surface skin temperature
- Updated ozone profile with GISS ozone and MEaSUREs GOZCARDS.
- Updated maps of surface topography, vegetation type, and snow/ice by ISCCP.

The purpose of this study is to explore the effect of the changes of clouds and meteorology on longwave fluxes at the surface and TOA.

2. Data Sources

The nnHIRS data are the HIRS temperature and water vapor retrievals (Shi et al., 2012) that are further processed by the ISCCP team to produce globally filled 3-hourly data products.

The cloud properties are beta products from the next version of ISCCP data (called H Series) that provide radiances and cloud/surface retrievals for all 8-10 km pixels include in ISCCP B1 (previous version subsampled to 30 km). Satellite calibration and cloud retrievals have been updated and an additional cloud type of high water clouds has been added to the properties.

The Princeton land surface temperature (PLST) data uses a process that adjusts output from the NCEP Climate Forecast System Reanalysis (CFSR) with satellite retrievals from HIRS analysis and then used to force the VIC macroscale model (Coccia et al., 2013). The Seaflux sea surface temperature is based on AVHRR data that has been adjusted with a daytime curve for diurnal variation (Clayson and Bogdanoff, 2012).

MERRA-2/GEOS-4 are reanalysis products from the GMAO, providing temperature and humidity values for the purpose of this study as inputs to the longwave algorithm.

RSS profile temperatures and column water vapor are created with microwave sounder data from MSU and AMSU instruments (Mears and Wentz, 2009 (2) and Mears, Schabel and Wentz, 2003). NVAP-M water vapor retrievals were also based in part upon microwave and also used additional satellite and radiosonde data sets (VonderHaar et al., 2012).

CERES SYN1deg computes fluxes with the Langley Fu-Liou radiative transfer model (used here for the Rel. 4 longwave fluxes) and constrained by the observed CERES TOA fluxes (Doelling et al., 2013; Rose et al., 2013). CERES Energy Balanced and Filled (EBAF) data is based on the SYN1deg product (Loeb et al., 2009; Kato et al., 2012). The EBAF long-term global averaged global net TOA fluxes and components are constrained to the ocean heat storage estimated from ocean buoy measurements using uncertainty information of the atmospheric constituents and surface properties.

3. Flux Comparisons as a Result of Differing Cloud Inputs

Here we isolate the flux differences that result from changing the cloud properties that are input into the longwave flux algorithm. First presented are map differences of ISCCP DX and HX cloud properties, then flux differences. The same profile and surface meteorology are used in each case for the flux differences shown at the bottom. The longwave algorithm uses IR-only cloud properties for night-time calculations and VIS-adjusted/IR cloud properties during the day. All maps are annual average difference maps for 2007. Global and and 20°N-20°S (in parentheses) areal averages are given in tables for cloud properties.

Total Cloud

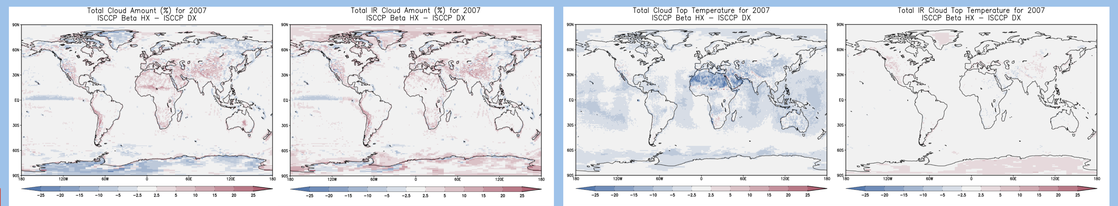

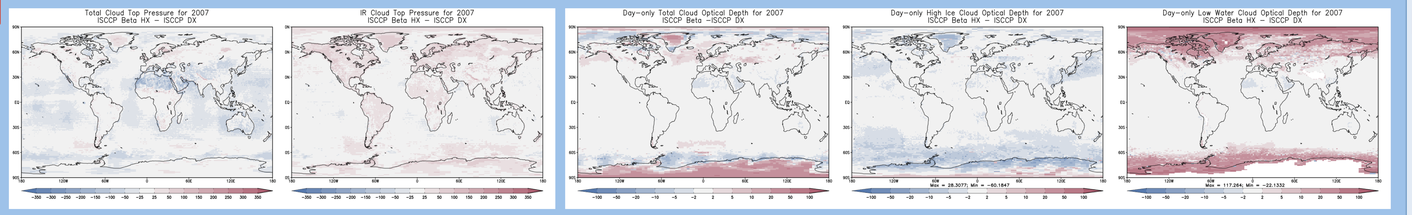

VIS Cloud Top Temperature

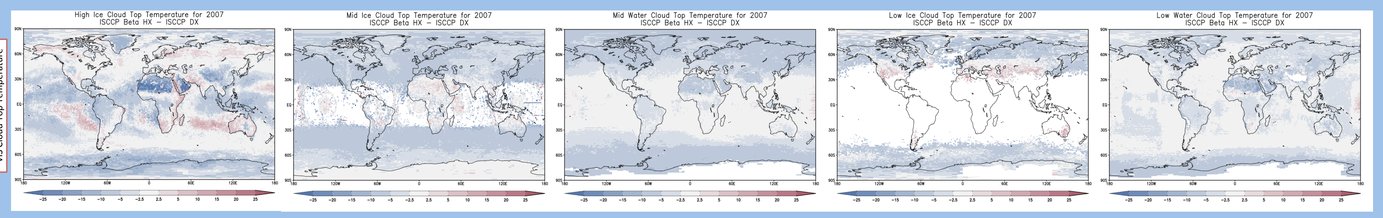

IR-only Nighttime Cloud Top Temperature

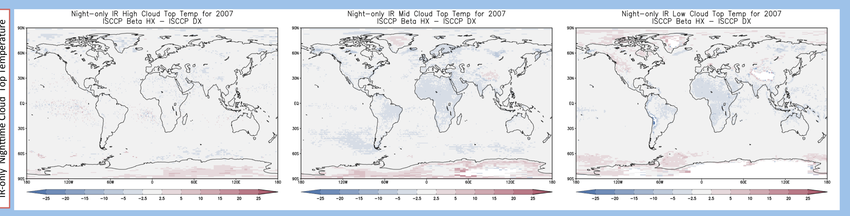

Longwave Fluxes

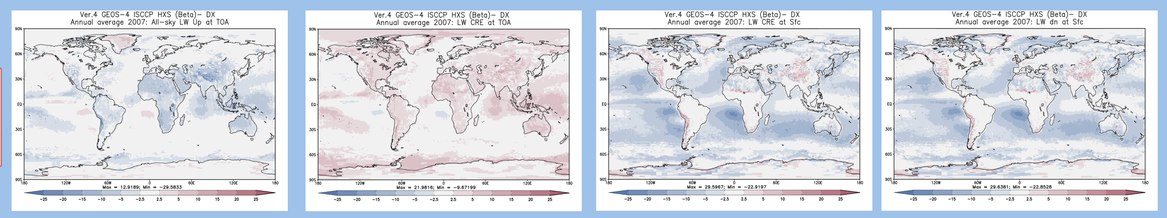

Table 1: Global and 20°N-20°S (in parentheses) areal annual averages of 2007 for total cloud (visible + IR) and IR-only cloud properties. While not directly used in the calculation of longwave fluxes, they are presented for comparison of the total cloud properties.

	Total Cloud		IR-only Total Cloud	
	HX	DX	HX	DX
Amount (%)	63.4 (57.5)	62.8 (56.9)	61.4 (55.2)	60.3 (54.6)
Top Temperature (K)	261.5 (267.7)	264.4 (271.4)	269.6 (278.5)	269.6 (279.0)
Top Pressure (hPa)	610.2 (611.5)	628.5 (634.0)	679.9 (694.8)	670.6 (692.3)

Table 2: Global and 20°N-20°S (in parentheses) areal annual averages of 2007 for day-time only (visible) cloud. These are the properties used for day-time calculations of longwave fluxes.

	High Ice		High Wat	Mid Ice		Mid Water		Low Ice		Low Water	
	HX	DX	HX	HX	DX	HX	DX	HX	DX	HX	DX
Amount (%)	27.7 (29.2)	20.9 (25.4)	0.71 (1.26)	5.0 (0.02)	10.5 (0.54)	11.4 (9.7)	10.4 (12.3)	0.23 (0.002)	1.74 (0.0)	21.2 (19.4)	22.0 (20.7)
Top Temperature (K)	219.9 (214.4)	223.1 (218.9)	254.3 (255.9)	250.9 (260.0)	257.0 (262.6)	265.8 (271.6)	269.0 (272.8)	257.3 (280.2)	259.8 (269.2)	278.1 (286.8)	280.9 (289.1)
Optical Depth	5.10 (3.17)	5.76 (3.62)	14.4 (15.2)	7.30 (0.18)	4.36 (0.46)	16.87 (5.28)	9.22 (5.13)	4.34 (0.02)	1.92 (0.0)	12.4 (3.66)	7.97 (4.1)

Table 3: Global and 20°N-20°S (in parentheses) areal annual averages of 2007 for night-time only (IR) cloud. These are the properties used for night-time calculations of longwave fluxes.

	High IR (night-only)		Mid IR (night-only)		Low IR (night-only)	
	HX	DX	HX	DX	HX	DX
Amount (%)	13.5 (15.6)	13.8 (15.6)	21.8 (15.0)	22.7 (15.8)	25.9 (25.4)	23.9 (24.0)
Top Temperature (K)	239.6 (244.1)	240.2 (244.6)	263.8 (272.6)	265.3 (274.3)	278.2 (287.7)	279.5 (289.8)

4. Flux Comparisons as a Result of Differing Meteorological Inputs

In this section we isolate the flux differences that result from changing meteorological profiles. The flux differences shown here are holding the cloud properties constant by only using the ISCCP HX data. In addition to comparing different meteorological data sets that have been used in the longwave algorithm, we compare integrated temperature and moisture fields from RSS and NVAP-M.

Integrated Profile Temperature

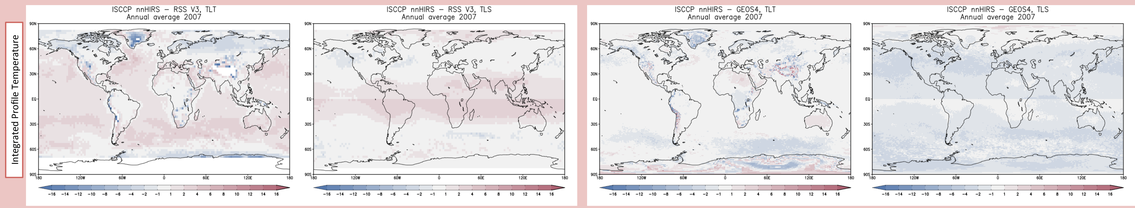

Table 4: : Global and 20°N-20°S (in parentheses) areal annual averages of 2007 for integrated profile. The integrations are based on weights given by the RSS team (Mears and Wentz, 2009).

	nnHIRS	GEOS-4	MERRA-2	RSS
Temp Lower Troposphere	269.9 (280.1)	270.2 (280.3)	270.0 (280.2)	270.5 (279.2)
Temp Lower Stratosphere	210.8 (205.6)	212.3 (206.8)	213.3 (208.2)	210.0 (203.7)

Integrated Water Vapor

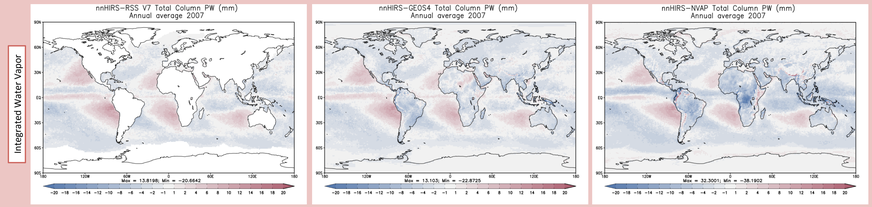

Table 5: Global and 20°N-20°S (in parentheses) areal annual averages of 2007 for total column water. The first row of values gives values for the combined land and ocean, while the second row is only over ice-free ocean areas defined by the RSS data set.

	nnHIRS	GEOS-4	NVAP	MERRA-2	RSS
Land and Ocean	23.5 (39.4)	24.5 (40.2)	25.5 (42.6)	24.9 (40.8)	
Ocean Only	29.0 (42.0)	29.3 (41.8)	30.7 (44.2)	29.5 (42.0)	29.6 (42.3)

Longwave Fluxes

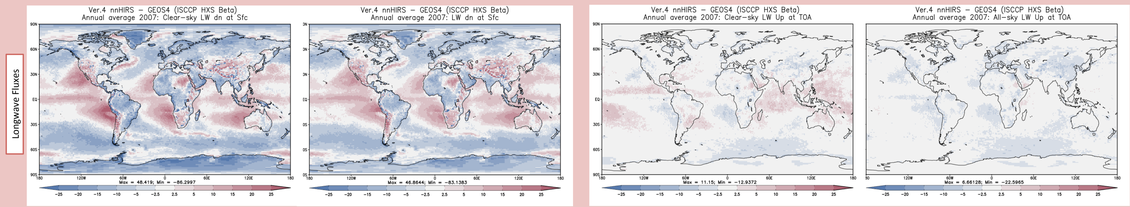

5. Summary and Validation of Fluxes from Various Inputs

Table 6: Global and 20°N-20°S (in parentheses) areal annual averages of 2007 for Surface Down, Outgoing Longwave Radiation (OLR) and Cloud Radiative Effect (CRE) global and 20°N-20°S areal annual averages of 2007. Note that clear-sky (aerosols, but no clouds) and pristine-sky (no clouds and no aerosol fluxes) are also given.

	Rel. 4 nnHIRS /Beta	Rel. 4 GEOS-4/Beta	Rel. 4 MERRA-2/Beta	Rel. 4 GEOS-4 /DX	Rel. 3.1 GEOS-4 /DX *	CERES EBAF Ed. 2.8	CERES SYN 1-deg
Sfc Down	344.2 (405.1)	345.1 (405.6)	344.9 (406.1)	348.5 (409.2)	344.8 (404.5)	345.5 (403.9)	341.8 (399.3)
Clear Sfc Down	313.8 (390.4)	315.9 (388.7)	316.2 (389.3)	315.7 (388.7)	311.4 (383.4)*	316.8 (390.7)	314.3 (386.0)
Prist. S. Dn	312.4 (389.1)	314.5 (387.3)	314.8 (388.0)	314.3 (387.3)			
Sfc CRE	30.4 (17.7)	29.2 (17.0)	28.7 (16.7)	32.8 (20.5)	33.4 (21.1)	28.7 (13.2)	27.5 (13.3)
OLR	233.5 (251.7)	235.0 (252.5)	234.4 (251.8)	236.9 (255.4)	238.3 (256.6)	240.0 (256.7)	238.7 (255.2)
Clear OLR	264.1 (285.7)	264.1 (284.4)	262.7 (282.7)	263.8 (284.5)	265.3 (285.9)*	266.0 (286.6)	266.3 (287.5)
Prist. OLR	265.4 (287.0)	265.3 (285.5)	263.8 (283.8)	264.9 (285.6)			
TOA CRE	30.6 (34.0)	29.1 (31.9)	28.3 (30.9)	26.8 (29.2)	27.0 (29.3)	26.0 (29.9)	27.6 (32.3)
					* No aerosol		

Table 6 gives the global and tropical (20°N-20°S) areal averages for the annual average of 2007. For comparison to similar data sets, the averages for CERES EBAF and SYN1deg data are also presented.

BSRN and PMEL Validation

Table 7: BSRN and PMEL validation of surface downwelling longwave flux for release 3.1 and 4.0 for the monthly averaged fluxes.

		Bias	RMS	ρ	σ	μ_{LW}	N
Rel. 4 nnHIRS/Beta	BSRN	2.36	17.57	0.9767	17.42	308.94	464
	PMEL	7.76	10.38	0.8806	6.97	414.71	50
Rel. 4 GEOS-4/Beta	BSRN	4.26	13.81	0.9864	13.15	310.84	464
	PMEL	-0.10	6.97	0.9397	7.01	406.84	50
Rel.4 MERRA-2/Beta	BSRN	5.21	13.78	0.9871	12.77	311.79	464
	PMEL	-1.03	7.65	0.9462	7.66	405.91	50
Rel. 4 GEOS-4/DX	BSRN	4.88	13.75	0.9870	12.86	311.46	464
	PMEL	4.43	7.30	0.9371	5.86	411.39	50
Rel. 3.1 GEOS-4/DX	BSRN	2.09	12.30	0.9882	12.23	308.08	464
	PMEL	-0.07	6.17	0.9342	6.23	406.88	50
CERES EBAF Ed. 2.8	BSRN	1.01	10.02	0.9922	9.98	308.12	464
	PMEL	-2.12	5.10	0.9297	4.69	404.82	50
CERES SYN 1-deg	BSRN	-3.66	10.29	0.9927	9.62	303.44	464
	PMEL	-2.95	5.57	0.9285	4.77	403.99	50

Table 7 gives the monthly averaged surface downwelling validation statistics for land observations from BSRN and ocean buoy observations from PMEL. For comparison to similar data sets, the statistics for CERES EBAF and SYN1deg data are also presented.

6. Flux Comparisons as a Result of Differing Both Clouds and Meteorological Conditions

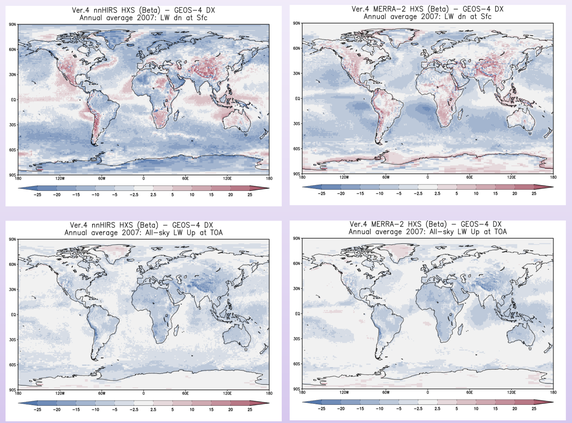

7. Conclusions

This poster highlights the ongoing assessments made of the sensitivity of GEWEX/SRB longwave radiative transfer algorithm to changes in key inputs including upgraded new ISCCP clouds and new ISCCP HIRS analysis.

In looking at how meteorological changes affect fluxes, the largest sensitivity for downward flux at the surface is atmospheric water vapor. The patterns of flux differences almost directly mirror those of the patterns of differences of the total column water vapor (TCWV), particularly over oceans. The ISCCP nnHIRS appears to be much more moist in sub-tropical subsidence areas corresponding to major stratocumulus regions. Clear-sky OLR shows slight negative correlation with the TCWV, but is also affected by upper-atmosphere temperatures.

The comparison to ocean buoys appear to confirm the finding and show a large positive bias (most ocean buoys are in the tropical oceans). There is a smaller bias over land sites where BSRN are located. RMS differences and correlations relative to BSRN and buoys are significantly worse when using nnHIRS than GLW v3.1 for the test versions here.

Cloud top temperatures are the driving force of the differences seen in this study. The day-time VIS clouds are much colder in the new ISCCP HX version of clouds than the previous DX version. Therefore the OLR fluxes have decreased significantly. Comparisons to CERES data set indicates a divergence from CERES in these test versions relative to version 3.1.

References

Clayson and Bogdanoff, 2013: The Effect of Diurnal Sea Surface Temperature Warming on Climatological Air-Sea Fluxes. J. Climate, 26,2546-2556.

Coccia et al., 2013: Creating a Global Land Surface Temperature Dataset Combining HIRS Retrievals and Land Surface Model Simulations Through Bayesian Uncertainty Post-Processing. AGU Fall Meeting.

Doelling et al., 2013:Geostationary Enhanced Temporal Interpolation for CERES Flux Products. . J. Atmos. Oceanic Technol., 30,1072-1090.

Kato et al, 2012: Surface Irradiances Consistent with CERES-Derived Top-of-Atmosphere Shortwave and Longwave Irradiances. *J. Climate*, 26, 2719-2740.

Loeb et al., 2009: Toward Optimal Closure of the Earth's Top-of-Atmosphere Radiation Budget. J. Climate, 22, 748-766.

Mears, C.A., M. Schabel, and F.J. Wentz, 2003: A Reanalysis of the MSU Channel 2 Tropospheric Temperature Record. *J. Climate*, 16, 3650-3664.

Mears, C. A. and F. J. Wentz, (2009) Construction of the Remote Sensing Systems V3.2 Atmospheric Temperature Records From the MSU and AMSU Microwave Sounders, . J. Atmos. Oceanic Technol, 26, 1040-1056.

Mears, C. A. and F. J. Wentz, (2009) Construction of the RSS V3.2 Lower Tropospheric Dataset From the MSU and AMSU Microwave Sounders, . J. Atmos. Oceanic Technol., 26, 1493-1509.

Rose et al., 2013: An Algorithm for the Constraining of Radiative Transfer Calculations to CERES-Observed Broadband Top-of-Atmosphere Irradiance. *J. Atmos. Oceanic Technol.*, 30, 1091–1106.

Rose et al., 2006: CERES Proto-Edition3 Radiative Transfer: Model Tests and Radiative Closure Over Surface Validation Sites. 12th AMS Conference on Atmospheric Radiation, Madison WI.

Shi, Lei, Ge Peng, John J. Bates, 2012: Surface Air Temperature and Humidity from Intersatellite-Calibrated HIRS Measurements in High Latitudes. J. Atmos. Oceanic Technol., 29, 3–13.

Stackhouse et al., 2011: The NASA/GEWEX Surface Radiation Budget Release 3.0: 24.5-Year Dataset. *GEWEX News*, 21, No. 1, February, 10-12.

Vonder Haar, T. H., J. L. Bytheway, and J. M. Forsythe (2012), Weather and climate analyses using improved global water vapor observations, Geophys. Res. Lett., 39, L15802, doi: 10.1029/2012GL052094.

Acknowledgements

This work was supported by NASA's Science Mission Directorate under the Dr. Jack Kaye and Radiation Sciences Program administered by Dr. Hal Marring.

The GEWEX SRB website is http://gewex-srb.larc.nasa.gov/ . A link to order Rel. 3.1 data is available through the website.